CO_2 Removal from Multi-component Gas Mixtures

Utilizing Spiral-Wound Asymmetric Membranes

*** W. B. Said, ** M. F. M. Fahmy, *** F. K. Gad, *** G. A. El-Aleem**

ABSTRACT

A systematic procedure and a computer program have been developed for simulating the performance of a spiral-wound gas permeator for the CO_2 removal from natural gas and other hydrocarbon streams. The simulation program is based on the approximate multi-component model derived by Qi & Henson[1], in addition to the membrane parameters achieved from the binary simulation program[2] (permeability and selectivity). Applying the multi-component program on the same data used by Qi & Henson to evaluate the deviation of the approximate model from the basic transport model, showing results more accurate than those of the approximate model, and are very close to those of the basic transport model, while requiring significantly less than 1% of the computation time. The program was successfully applied on the data of Salam gas plant membrane unit at Khalda Petroleum Company, Egypt, for the separation of CO_2 from hydrocarbons in an eight-component mixture to estimate the stage cut, residue, and permeate compositions, and gave results matched with the actual Gas Chromatography Analysis measured by the lab.

* Khalda Petroleum Company, Egypt.
** Chemical Engineering Department, Faculty of Engineering, Cairo University.
*** Faculty of Petroleum & Mining Engineering, Suez Canal University.

1. INTRODUCTION

In recent years, gas separation membranes have emerged as a viable alternative to more mature technologies such as absorption and cryogenic distillation. The use of spiral-wound permeators to separate gas mixtures encountered in natural gas treatment and enhanced oil recovery is one of the most important applications of membrane technology. However, the lack of appropriate permeators models, and hence simulation programs is a major obstruction to effective simulation and design of membrane processes.

To exploit the use of membranes fully, the engineer must have access to appropriate software tools necessary to integrate membranes for an optimized system. While software models exist for membrane unit operations, the performance and costs generally are available only from commercial membrane vendors, typically on a case-by-case basis. Therefore, the engineer may not readily be able to fully explore the options necessary to determine the optimum process configuration for the specific gas stream to be treated.

Like any process, membrane units are designed to handle feed streams with specific operating conditions. By the time, most of the operating conditions become different from the design basis to some extent. For example:

1- Slight variations in inlet feed composition. These variations may be due to that, plant feed consists of different sources, which have different

CO_2 concentrations. The reduction in one or more sources will affect the feed composition obviously.

2- Occasional Variations in the export gas rate (residue) due to different nominations from pipeline authority, which depend on the end consumers need.

3- The normal and abnormal decline in permeators' efficiency

In addition, an optimization should be made between the product specification and hydrocarbon losses (e.g., to be on spec., CO_2 content should be < 3.0 mole%. Although one might think that export gas of 2.8 mole% CO_2 content will be better, but this mean flaring more hydrocarbons). Hence, the operation staff is in acute need for an effective simulation program to monitor the membrane performance, and set the optimum operating conditions that can verify the highest on spec. gas production with minimum hydrocarbon losses. The major obstructions against that goal are:

1- Unavailability of element configuration data, which considered a proprietary of the manufacturer.
2- The lack of appropriate permeator models (especially multi-component models).

2. METHOD OF CALCULATION

Figure 1 illustrates the permeation process through an extended membrane leaf. The same figure was used by Qi & Henson to derive the basic transport model. Calculation for multi-component approach is based mainly on the membrane parameters achieved from the binary simulation

program[2] (permeability and selectivity). These results will not be used directly as it is, but it need some additional processing as follow:

a) Permeability (Q_b/d) obtained from the Binary program calculations is the average value for C_1+. In order to obtain the value of (Q_b/d) of C_1 only, an approximate composition factor should be calculated using the compositions and selectivities of the feed components excluding CO_2. Equation (1) shows how to calculate this factor.

$$Composition\ Factor = \sum_{i=1}^{n-1} \frac{x_{i,f}}{1 - x_{CO2}} \alpha_i \qquad (1)$$

where α_{C1} is equal to unity (C_1 is the base component), and other components selectivities are: α_{N2} = (5/6), α_{C2} = (1/2), α_{C3} = (1/3), α_{C4} = (1/4), α_{C5} = (1/5), and α_{C6+} = (1/6), as stated in most vendors' manual[3] for cellulose acetate.

b) Since, in multi-component program we use N_2 as the base component, final substitutive values of (Q_b/d) and α_{CO2} will be as follow:

$$(Q_b/d)_{\text{multi-comp.}} = \frac{(Q_b/d)_{\text{binary}} \times (5/6)}{\text{Composition Factor}} \qquad (2)$$

$$(\alpha_{CO2})_{\text{multi-comp.}} = \frac{(\alpha_{CO2})_{\text{binary}} \times \text{Composition Factor}}{(5/6)} \qquad (3)$$

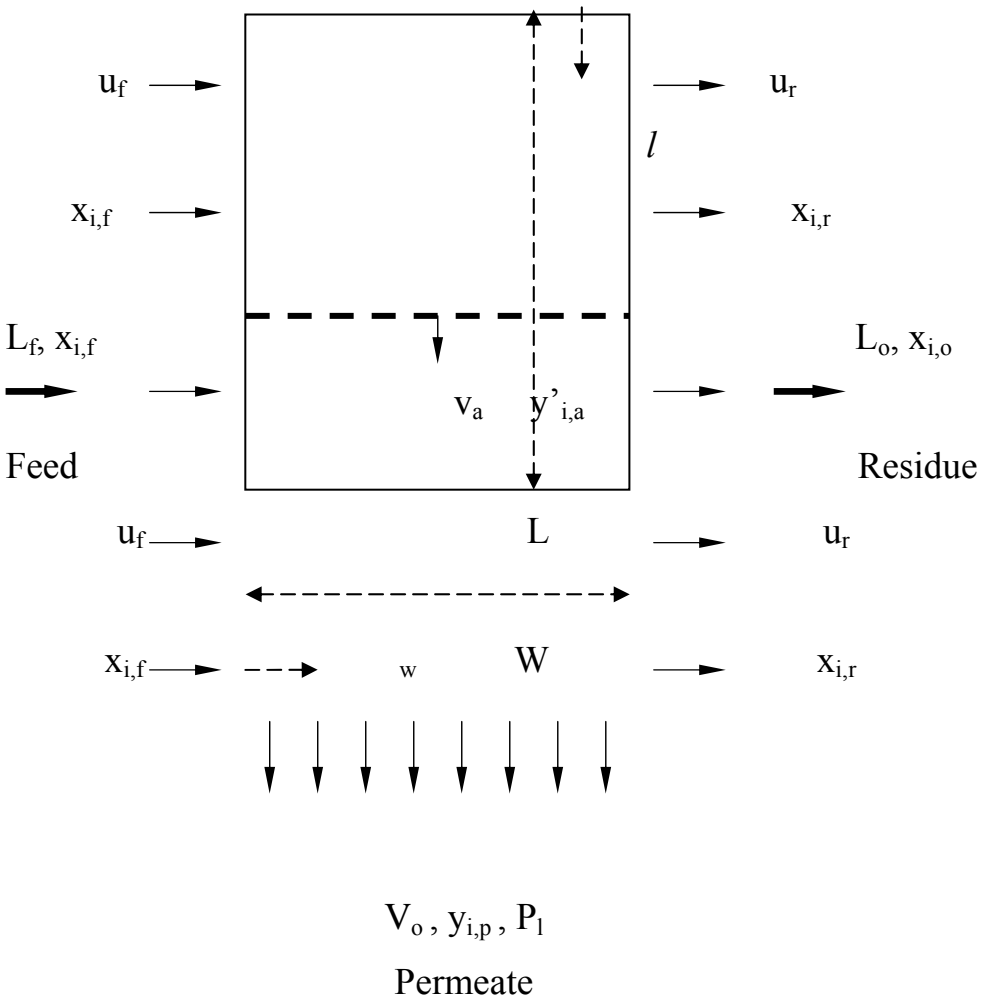

Figure 1. Gas permeation through an extended spiral-wound membrane leaf

2.1 Calculation Procedure: -

1- The following variables must be known to start the calculations: (T_f, x_{if}, α_i, (Q_b/d), P_h, P_l, q_f, μ, N_P, N_S, N_L, t, W, L, and B).

2- The value of L_f in kg-mol/s is calculated using equation (4)

$$L_f = \frac{(24)(1762)q_f}{(10^6)(3600)N_P N_L} \tag{4}$$

3- The value of C & R are calculated using equations (5) and (6) respectively.

$$C = \frac{2R_g T\mu L^2 u_f}{g_c WtBP_h{}^2} = \frac{2R_g T\mu LL_f}{g_c WtBP_h{}^2} \tag{5}$$

$$R = \frac{2Q_b WP_h}{du_f} = \frac{2Q_b LWP_h}{dL_f} \tag{6}$$

4- For a leaf length variable h = 0, the pressure ratio γ is calculated using equation (7).

$$\gamma^2 = \gamma_o^2 + \frac{1}{2}C(1-U_r)(1-h^2) \tag{7}$$

Note: $\gamma_o = (P_l/P_h)$

5- For a given $x_{i,f}$, equation (8) is solved for $y'_{m,f}$

$$\sum_{i=1}^{n} \frac{\alpha_i x_i y'_m}{1-\gamma+\gamma\alpha_i y'_m} = 1 \tag{8}$$

6- The value of $y'_{i,f}$ is calculated using equation (9)

$$y'_i = \frac{\alpha_i x_i y'_m}{1-\gamma+\gamma\alpha_i y'_m} \tag{9}$$

7- The value of U_r and $y'_{i,r}$ are obtained by integrating the initial-value differential equations (10) and (11), and simultaneous solution with equation (13). Numerical solutions are obtained by

using a fourth-order Runge–Kutta–Gill approximation at each quadrature point $y'_{m,j}$ and the outlet point $y'_{m,r}$ (equation – 12).

$$\frac{d(\ln U)}{dy'_m} = -\frac{\sum_{j=1}^{n} A_j y'_j}{\sum_{j=1}^{n} B_j y'_j} \tag{10}$$

where

$$A_j = \frac{1-\gamma}{(1-\gamma+\gamma\alpha_j y'_m)y'_m}$$

$$B_j = \frac{(1-\gamma)(\alpha_j y'_m - 1)}{1-\gamma+\gamma\alpha_j y'_m}$$

$$\frac{dy'_i}{dy'_m} = y'_i\left(A_i - \frac{B_i\sum_{j=1}^{n} A_j y'_j}{\sum_{j=1}^{n} B_j y'_j}\right), \qquad i = 2,...,n \tag{11}$$

$$Y_j = Y_{j-1} + \frac{1}{6}(K_1 + K_4) + \frac{1}{3}(\lambda_2 K_2 + \lambda_4 K_3) \tag{12}$$

where

$$K_1 = \delta_j F(y'_{m,j-1}, Y_{j-1})$$

$$K_2 = \delta_j F\left((y'_{m,j-1} + \frac{\delta_j}{2}), (Y_{j-1} + \frac{1}{2}K_1)\right)$$

$$K_3 = \delta_j F\left((y'_{m,j-1} + \frac{\delta_j}{2}), (Y_{j-1} + \lambda_1 K_1 + \lambda_2 K_2)\right)$$

$$K_4 = \delta_j F\left((y'_{m,j-1} + \delta_j), (Y_{j-1} + \lambda_3 K_2 + \lambda_4 K_3)\right)$$

Where

$$Y_j = \left[\ln U_j, y'_{2j}, ..., y'_{nj}\right]^T$$

$$F = \left[f_U, f_2, ..., f_n\right]^T$$

$$\delta_j = y'_{m,j} - y'_{m,j-1}$$

$$\lambda_1 = \frac{\sqrt{2}-1}{2},\ \lambda_2 = \frac{2-\sqrt{2}}{2},\ \lambda_3 = -\frac{\sqrt{2}}{2},\ \lambda_4 = \frac{2+\sqrt{2}}{2}$$

The functions $f_U, f_2, \ldots, f_n$ represent the right-hand sides of (10) and (11), and $y'_{i,j}$ represents the permeate concentration of the *i*th component at the quadrature point $y'_{m,j}$. The initial conditions are:

$$Y_0 = \left[0, y'_{2,f}, ..., y'_{n,f}\right]^T$$

$$R = \frac{1}{1-\gamma}(y'_{m,f} - U_r y'_{m,r} + (y'_{m,r} - y'_{m,f})\sum_{j=1}^{N} U_j w_j) \qquad (13)$$

8- The value of $x_{i,r}$ is then calculated using equation (14).

$$x_i = \gamma y'_i + \frac{(1-\gamma)y'_i}{\alpha_i y'_m} \qquad (14)$$

9- By performing a material balance on a differential length of membrane, $y'_{i,a}$ is calculated using equation (15).

$$y'_{i,a} = \frac{x_{i,f} - x_{i,r}U_r}{1-U_r}, \qquad i = 2, ..., n \qquad (15)$$

10- Steps from 4 to 9 are then repeated for h = 0.5 and h = 1.

11- The value of θ_o is then calculated from equation (16) using Simpson's rule.

$$\theta_0 = 1 - \int_0^1 U_r \cong 1 - \frac{0.5}{3}\left[U_r(h=0) + 4U_r(h=0.5) + U_r(h=1)\right] \qquad (16)$$

12- The value of $y_{i,p}$ is then calculated from equation (17) using Simpson's rule.

$$y_{i,p} = \int_0^1 y'_{i,a}\, dh \cong \frac{0.5}{3}\left[y'_{i,a}(h=0) + 4y'_{i,a}(h=0.5) + y'_{i,a}(h=1)\right], \quad i = 2,...,n \tag{17}$$

13- Writing an overall material balance around the membrane, The value of $x_{i,o}$ can be calculated from equation (18).

$$x_{i,o} = \frac{x_{i,f} - \theta_0 y_{i,p}}{1 - \theta_0} \tag{18}$$

3. CASE STUDY

The validity of the multi-component simulation program was tested by comparing the results obtained from it, with the actual existing operating parameters collected from the DCS and lab. G.C analysis of four samples taken from the feed, residue, and permeate streams of Salam gas plant membrane unit. **Tables (1) - (4)** summarize the input data, which contain the feed stream conditions and the required output data obtained from binary simulation program[2].

Table 1. Input Data for Sample 1.

Components	$x_{i,f}$	α_i	**C**	**R**
N_2	0.0070	1.00		
CO_2	0.0639	10.11		
C_1	0.7501	1.20		
C_2	0.1107	0.60		
C_3	0.0498	0.40		
C_4	0.0159	0.30		
C_5	0.0024	0.24		
C_6+	0.0002	0.20		
Total	1.0000		0.0306	0.1096

Table 2. Input Data for Sample 2.

Components	$x_{i,f}$	α_i	**C**	**R**
N_2	0.0070	1.00		
CO_2	0.0630	9.92		
C_1	0.7490	1.20		
C_2	0.1117	0.60		
C_3	0.0507	0.40		
C_4	0.0160	0.30		
C_5	0.0024	0.24		
C_6+	0.0002	0.20		
Total	1.0000		0.0310	0.1153

Table 3. Input Data for Sample 3.

Components	$x_{i,f}$	α_i	**C**	**R**
N_2	0.0090	1.00		
CO_2	0.0644	10.69		
C_1	0.7207	1.20		
C_2	0.1210	0.60		
C_3	0.0645	0.40		
C_4	0.0186	0.30		
C_5	0.0016	0.24		
C_6+	0.0002	0.20		
Total	1.0000		0.0258	0.1080

Fortunately, the first two samples were collected at different operating circumstances from the other two cases. The feed flow rate in Sample 2 is higher than the feed flow rate in Sample 3 by more than 48,500 (m^3/h {STP}).

Table 4. Input Data for Sample 4.

Components	$x_{i,f}$	α_i	C	R
N_2	0.0089	1.00		
CO_2	0.0663	10.38		
C_1	0.7251	1.20		
C_2	0.1180	0.60		
C_3	0.0621	0.40		
C_4	0.0178	0.30		
C_5	0.0015	0.24		
C_6+	0.0003	0.20		
Total	1.0000		0.0269	0.1147

4. RESULTS & DISCUSION

A comparison between the rest of the actual data and calculation results obtained according to the multi-component simulation program for these samples are summarized in the following tables:

Table 5. Comparison between actual operating data & calculated results obtained from multi-component simulation program for Sample 1.

Comp.	$y_{i,p}$		$x_{i,o}$		θ_o	
	Actual	Calc.	*Actual*	Calc.	Actual	Calc.
N_2	0.0062	0.0053	0.0072	0.0073		
CO_2	0.2606	0.2538	0.0303	0.0326		
C_1	0.6788	0.6683	0.7602	0.7636		
C_2	0.0438	0.0523	0.1239	0.1203		
C_3	0.0084	0.0160	0.0571	0.0554		
C_4	0.0022	0.0039	0.0183	0.0179		
C_5	0.0000	0.0005	0.0028	0.0027		
C_6+	0.0000	0.0000	0.0002	0.0002		
Total	1.0000	1.0000	1.0000	1.0000	0.1459	0.1417

Table 6. Comparison between actual operating data & calculated results obtained from multi-component simulation program for Sample 2.

Comp.	$y_{i,p}$		$x_{i,o}$		θ_o	
	Actual	Calc.	*Actual*	Calc.	Actual	Calc.
N_2	0.0059	0.0054	0.0071	0.0073		
CO_2	0.2508	0.2447	0.0296	0.0318		
C_1	0.6887	0.6754	0.7581	0.7617		
C_2	0.0442	0.0535	0.1253	0.1217		
C_3	0.0083	0.0165	0.0583	0.0566		
C_4	0.0021	0.0040	0.0187	0.0181		
C_5	0.0000	0.0005	0.0027	0.0027		
C_6+	0.0000	0.0000	0.0002	0.0002		
Total	1.0000	1.0000	1.0000	1.0000	0.1510	0.1467

Table 7. Comparison between actual operating data & calculated results obtained from multi-component simulation program for Sample 3.

Comp.	$y_{i,p}$		$x_{i,o}$		θ_o	
	Actual	Calc.	Actual	Calc.	Actual	Calc.
N_2	0.0084	0.0068	0.0093	0.0093		
CO_2	0.2716	0.2657	0.0298	0.0318		
C_1	0.6563	0.6446	0.7314	0.7330		
C_2	0.0485	0.0573	0.1329	0.1313		
C_3	0.0122	0.0208	0.0732	0.0716		
C_4	0.0030	0.0045	0.0213	0.0209		
C_5	0.0000	0.0003	0.0019	0.0018		
C_6+	0.0000	0.0000	0.0002	0.0002		
Total	1.0000	1.0000	1.0000	1.0000	0.1510	0.1393

Table 8. Comparison between actual operating data & calculated results obtained from multi-component simulation program for Sample 4.

Comp.	$y_{i,p}$		$x_{i,o}$		θ_o	
	Actual	Calc.	Actual	Calc.	Actual	Calc.
N_2	0.0076	0.0068	0.0093	0.0093		
CO_2	0.2704	0.2642	0.0296	0.0319		
C_1	0.6615	0.6483	0.7362	0.7384		
C_2	0.0469	0.0560	0.1315	0.1288		
C_3	0.0110	0.0200	0.0711	0.0694		
C_4	0.0026	0.0044	0.0202	0.0201		
C_5	0.0000	0.0003	0.0018	0.0017		
C_6+	0.0000	0.0000	0.0003	0.0003		
Total	1.0000	1.0000	1.0000	1.0000	0.1524	0.1481

4.1 Analysis and Discussion

It is clear from the above tables that, the maximum relative error in the prediction of stage cut (θ_o) is <± 4.1%. In Permeate stream, the error in the prediction of C_1 content <± 1.8%, in CO_2 content is <± 2.5%, which is considered a high accuracy for such complicated calculations. But the error increases gradually from 20% like C_2 content up to 100% for the case of C_5 content. This is probably due to low concentration of such heavy hydrocarbons in permeate stream, in addition to the uncertainty in knowing its exact selectivities. For residue stream, the maximum relative error in the prediction of C_1 content is <± 0.5%; C_2, C_3 & C_4 content is <± 3%; C_5 content is <± 4%; and CO_2 content is <± 7.5%.

All presented curves have been generated applying the multi-component simulation program based on the actual permeation data of 1st stage skid-D of Salam membrane unit. **Figures (2)** & **(3)** illustrate the effect of permeation factor (R) on the outlet residue concentration (x_{io}). It is noticed that, as R increases, the residue concentration of the most permeable component (CO_2) decreases, while the concentration of the moderately permeable component (C_1) exhibits a slight maximum until certain value of R, after which C_1 concentration starts to decrease again, and the concentration of the least permeable component (C_3, C_4+) increases.

This is what actually happen in operation at low feed flow rates (higher R); because boundary layer effect starts to appear due to the reduction in the degree of mixing in the feed channels. At such conditions, a continuous, non-compensated depletion in the CO_2 content

of the gas layer adjacent to the membrane surface will strongly decrease CO_2 driving force, and hence permeation rate, and at the same time increase C_1 permeation rate. This is why operation at low flow rates is not favorable to minimize the hydrocarbon losses, and avoid the concentration of the heavy staff, which may cause condensation.

Figures (4) & **(5)** depict the variation of stage cut (θ_o), and residue CO_2 concentration with permeation factor (R) for different feed CO_2 concentrations. As R increases, stage cut increases and CO_2 content in residue stream decreases. For higher CO_2 feed content, θ_o increases due to increase in driving force of the most permeable component, and hence permeation rate.

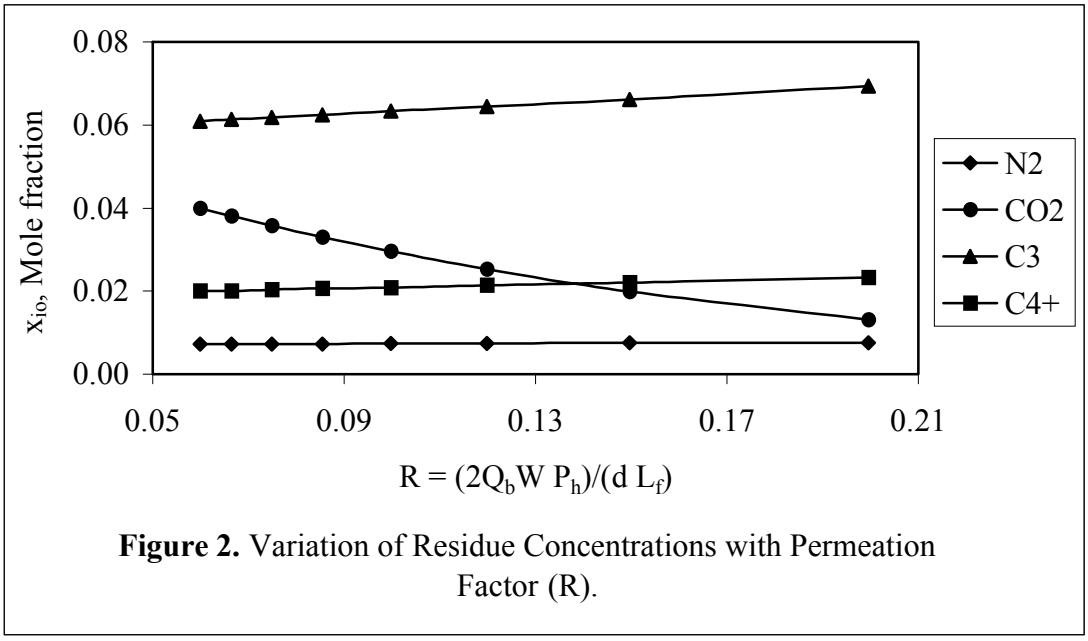

Figure 2. Variation of Residue Concentrations with Permeation Factor (R).

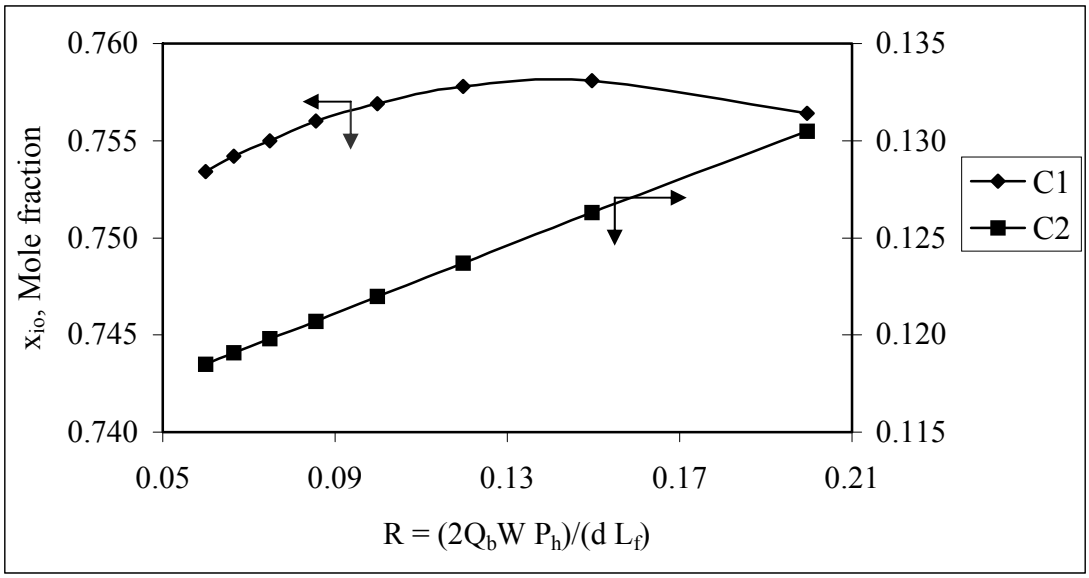

Figure 3. Variation of Residue Concentrations with Permeation Factor (R).

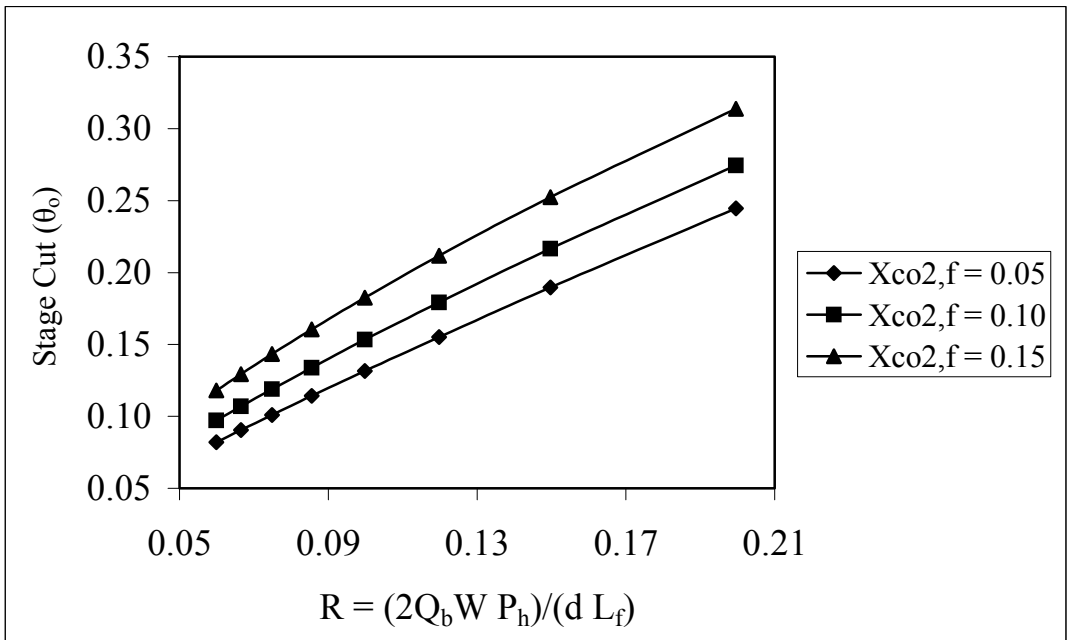

Figure 4. Effect of Feed Composition ($x_{CO2,f}$) on Stage Cut (θ_o)

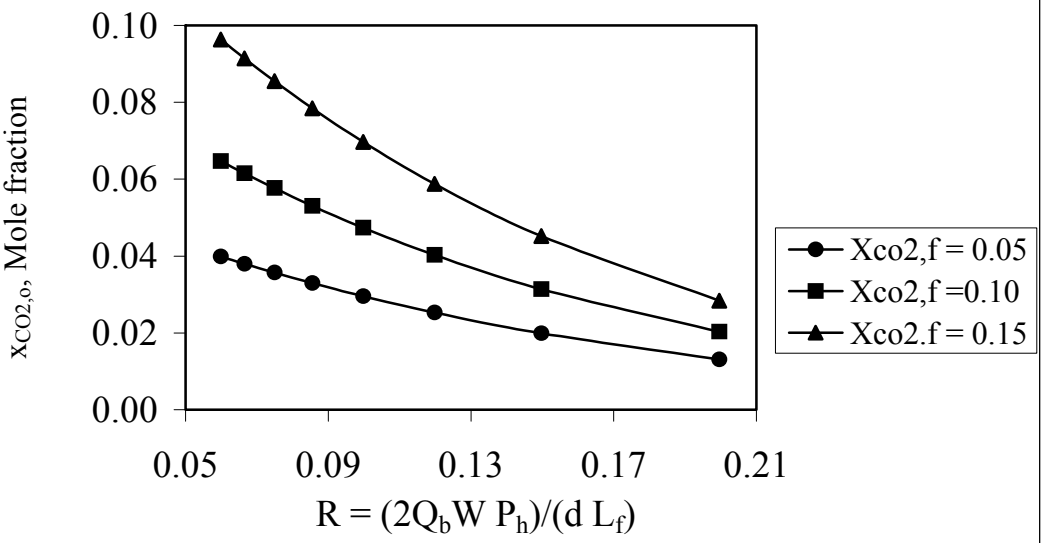

Figure 5. Effect of Feed Composition ($x_{CO2,f}$) on CO_2 Concentration in Residue Stream

Figures (6) & **(7)** illustrate the effect of changing the pressure ratio (γ_o) on the stage cut (θ_o), and CO_2 concentration in residue (x_{CO2}). It is noticed that, as the value of (γ_o) decreases, the stage cut (θ_o) slightly increases, while the residue concentration (x_{CO2}) decreases significantly.

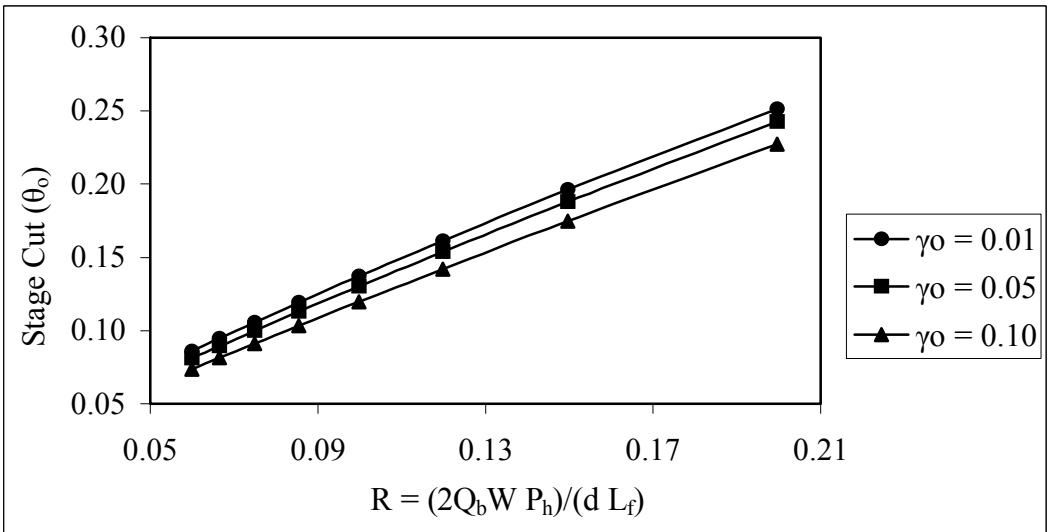

Figure 6. Effect of Pressure ratio (γ_o) on Stage Cut (θ_o)

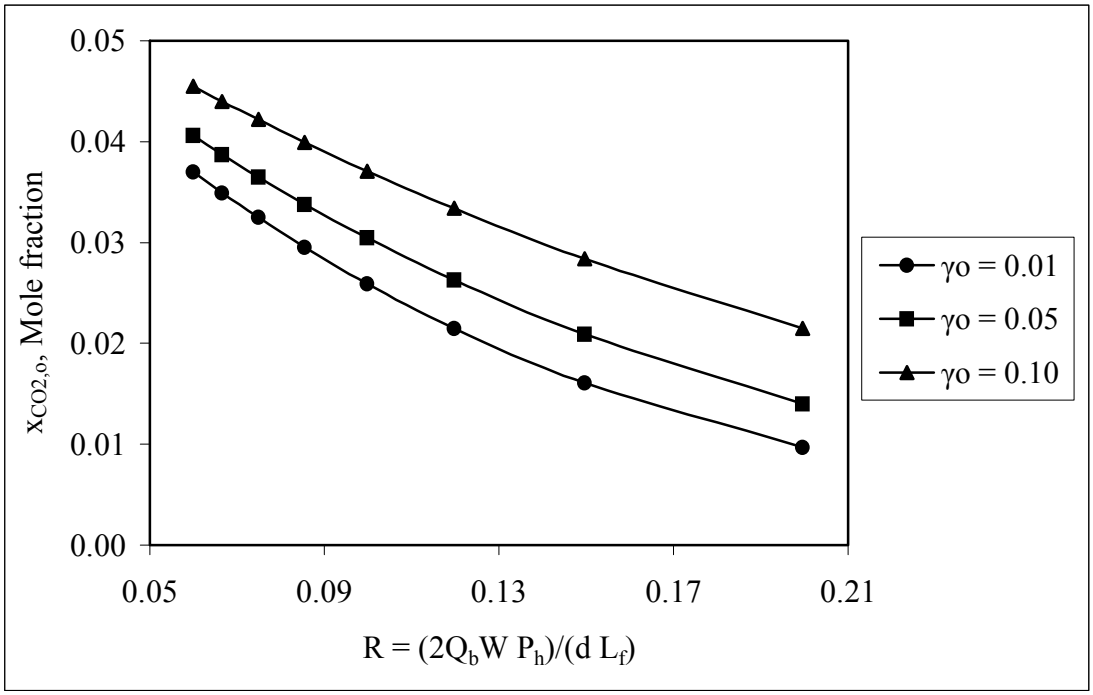

Figure 7. Effect of Pressure ratio (γ_o) on CO_2 Concentration in Residue Stream

Figures (8) & **(9)** illustrate the effect of selectivity on the stage cut (θ_o), and CO_2 concentration in residue (x_{CO2}). It is noticed that, the stage cut (θ_o) is slightly affected by the increase in α, while the residue concentration (x_{CO2}) decreases significantly. For that reason, the choice of using high selective material is a must, to achieve higher product purity with a tiny increase in permeation rate.

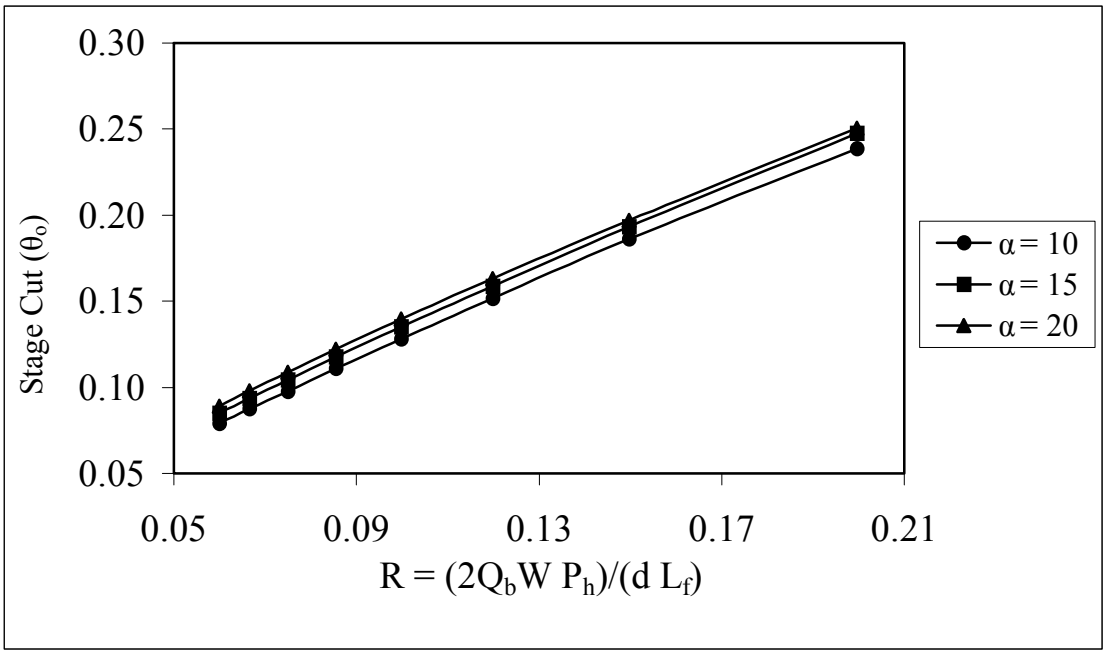

Figure 8. Effect of Selectivity for CO_2 (α_{CO2}) on Stage Cut (θ_o)

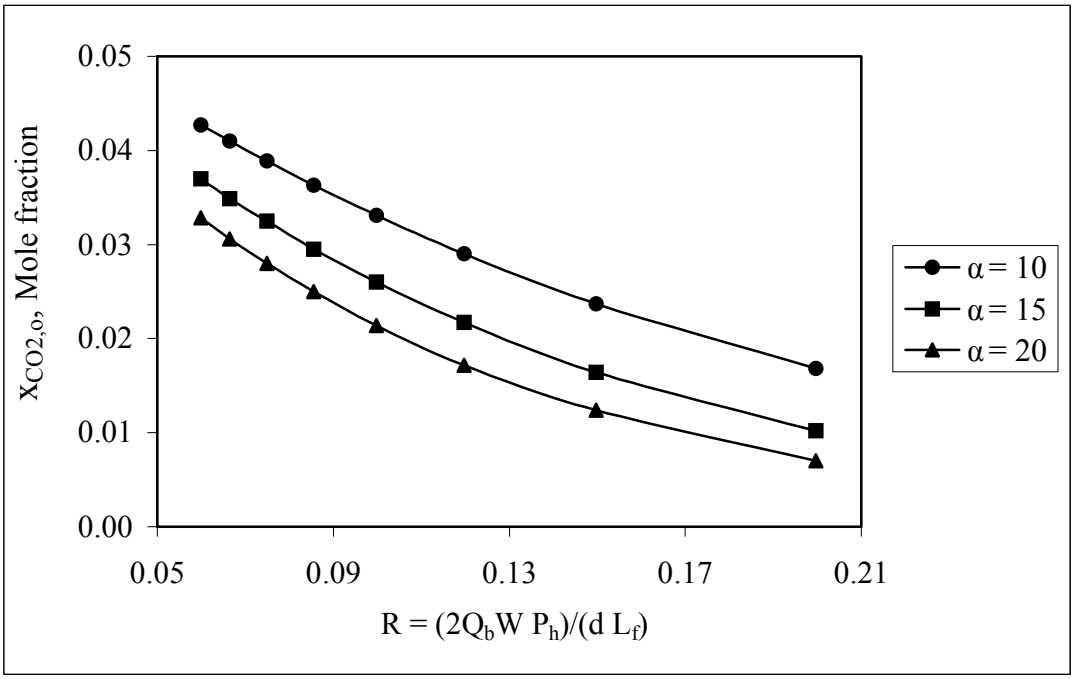

Figure 9. Effect of Selectivity for CO_2 (α_{CO2}) on CO_2 Concentration in Residue Stream

Furthermore, the accuracy of multi-component simulation program has been checked by applying the program on the same data used by Qi & Henson[1]. The data was used to evaluate the accuracy of the approximate model compared with the basic transport model. **Table 9** illustrates the comparison between the calculation results achieved in each case.

Table 9. Comparison between calculation results of Basic Transport Model (BTM), Approximate Model (APM), and Multi-Component Program (MCP)

Parameter	Value	Variable	BTM value	MCP value	APM value
$x_{i,f}$	0.20	$x_{i,o}$	0.0664	0.0660	0.0697
	0.20		0.1259	0.1256	0.1281
	0.20		0.1973	0.1973	0.1974
	0.20		0.2750	0.2753	0.2729
	0.05		0.0778	0.0779	0.0771
	0.05		0.0830	0.0831	0.0822
	0.05		0.0864	0.0865	0.0855
	0.05		0.0882	0.0883	0.0872
α_i	20	$y_{i,p}$	0.3724	0.3723	0.3723
	10		0.2957	0.2957	0.2951
	5		0.2035	0.2035	0.2035
	2		0.1032	0.1032	0.1036
	1		0.0141	0.0141	0.0142
	0.5		0.0074	0.0074	0.0074
	0.2		0.0030	0.0031	0.0031
	0.05		0.0008	0.0008	0.0008
γ_o	0.05	η_o	0.5634	0.5625	0.5694
C	0.1	θ_o	0.4366	0.4375	0.4306
R	0.1				

Although, multi-component simulation program is based on the approximate model, the results obtained according to its solution are very close to the results obtained using the basic transport model.

Consequently, the desired accuracy of basic transport model could be achieved by using multi-component program with less than 1% of the computation time required for the basic model.

5. CONCLUSION

The developed systematic procedure and the simulation program proved its ability to predict all the process parameters very quickly with an accepted error, in spite of the very complicated calculation steps included. Hence, Multi-component simulation program adopted is well suited for simulation and design of complex membrane separation systems, and it is expected that it will expand the public domain knowledge of the membranes in industry and facilitate the increased use of membranes for CO2 removal applications from natural gas.

6. NOMINCLATURE

B = permeability of the spacing materials inside the spiral wound leaf (m^2).

C = dimensionless constant defined by equation (5).

d = effective thickness of the membrane (m). ; g_c = Newton's law conversion factor.

$h = l/L$, dimensionless leaf length variable . ; l = membrane leaf length variable (m).

L = membrane leaf length (m). ; L_f = feed gas flow rate per membrane leaf (mol/s).

L_o = residue gas flow rate per membrane leaf (mol/s). ; P_h = feed-side pressure (Pa).

P_l = permeate outlet pressure (Pa).

Q_i = permeabilities of the ith permeable component (mol/m.s.Pa).

Q_b = permeability of the base component (mol/m.s.Pa).

R = dimensionless permeation factor defined by equation (6).

R_g = ideal gas constant (m^3.Pa/kg-mol.K) ; t = membrane leaf thickness (m)

T = temperature (^oK) ; $U = u/u_f$, dimensionless feed-side gas flow rate

U_j = dimensionless feed-side gas flow rate at jth quadrature point

$U_r = u_r/u_f$, dimensionless residue-side gas flow rate

u_f = feed gas flow rate per unit length of membrane leaf (mol/s.m)

u_r = residue gas flow rate per unit length of membrane leaf (mol/s.m)

V_o = permeate flow rate at permeate outlet (mol/s)

v_a = permeate flow rate per unit average over width of the membrane (mol/s.m)

W = membrane leaf width (m) ; w = membrane leaf width variable (m)

N_P = No. of parallel Feed streams ; N_S = No. of Membrane elements in series

q_f = Feed flow rate (m^3{STP}/h) ; x_i = Local feed-side concentration (mole fraction)

$x_{i,f}$ = Feed concentration (mole fraction)

$x_{i,o}$ = bulk residue stream concentration at outlet (mole fraction)

$x_{i,r}$ = local residue concentration along the outlet end of the membrane leaf

y_i = permeate concentration in bulk Permeate stream (mole fraction)

y_i' = local Permeate concentration on the membrane surface (mole fraction)

$y'_{i,a}$ = local Permeate concentration average over the width of the membrane (mole fraction)

$y'_{i,f}$ = local Permeate concentration along the inlet end of the membrane leaf (mole fraction)

$y'_{i,j}$ = local Permeate concentration at *j*th quadrature point (mole fraction)

$y'_{i,r}$ = local Permeate concentration along the outlet end of the membrane leaf

y'_m = composition variable ; $y'_{m,f} = y'_m$ value at the feed inlet

$y'_{m,r} = y'_m$ value at the residue outlet

$y_{i,p}$ = bulk Permeate stream concentration at permeate outlet (mole fraction)

$\alpha_i = Q_i/Q_b$,membrane selectivity for *i*th component

$\gamma = p/P_h$, *ratio of permeate pressure to feed pressure*

$\gamma_o = P_l/P_h$, *ratio of permeate pressure to feed pressure at permeate outlet*

μ = viscosity of gas mixture (Pa.s)

$\theta_o = V_o/L_f$, ratio of permeate flow rate to feed flow rate at permeate outlet (Stage cut)

$\eta_o = L_o/L_f$, ratio of residue outlet stream flow rate to feed flow rate

DCS = Distributed Control System

7. LITERATURE CITED

1. Qi, R.; Henson, M. A., "Approximate Modeling of Spiral-Wound Permeators", *Ind. Eng. Chem. Res.*, Vol. 36, Nov. 6, 1997.

2. W. B. Said, M. F. M. Fahmy, F. K. Gad, and G. A. El-Aleem, "CO_2 Removal from Natural Gas Utilizing Spiral-Wound Asymmetric Cellulose Acetate Membrane" , The 5th Egyptian Syrian Conference In Chemical & Petroleum Engineering, Vol. 1, pp. 60-73, 2003.

3. Lee, A. L., Feldkirchner, H. L., Stern, S. A., Houde, A. Y., Gamez, J. P., and Meyer, H. S., “Field Tests of Membrane Modules for the Separation of Carbon Dioxide From Low-Quality Natural Gas”, *Gas Sep. Purif*., Vol. 9, No. 1, pp. 35-45, 1995.